

# Recent advances in understanding diffusion in multi-principal element systems

Anuj Dash,<sup>1</sup> Alope Paul,<sup>1</sup> Sandipan Sen,<sup>2</sup> Sergiy Divinski,<sup>2</sup> Julia Kundin,<sup>3</sup> Ingo Steinbach,<sup>3</sup> Blazej Grabowski,<sup>4</sup> and Xi Zhang<sup>4</sup>

<sup>1</sup>Department of Materials Engineering, Indian Institute of Science, Bengaluru, India, 560012; email: aloke@iisc.ac.in

<sup>2</sup>Institute of Materials Physics, University of Münster, Münster, Germany, 48149

<sup>3</sup>ICAMS, Ruhr-University Bochum, Bochum, Germany

<sup>4</sup>Institute for Materials Science, University of Stuttgart, Stuttgart, Germany, 70569

Xxxx. Xxx. Xxx. Xxx. YYYY. AA:1–27

[https://doi.org/10.1146/\(\(please add article doi\)\)](https://doi.org/10.1146/((please add article doi)))

Copyright © YYYY by Annual Reviews.

All rights reserved

Posted with permission from

the Annual Review of Materials Research,

Volume 52 by Annual Reviews,

<http://www.annualreviews.org>.

## Keywords

diffusion, multi-principal element alloys, interdiffusion, *ab initio* simulations, CALPHAD approach, pair-exchange model (Max: 6 keywords)

## Abstract

Recent advances in the field of diffusion in multi-principal element systems are critically reviewed. Emphasis is put on experimental as well as theoretical approaches to determine atomic mobilities (tracer diffusion coefficients) in such chemically-complex multi-component systems. The newly elaborated, augmented pseudo-binary and pseudo-ternary methods provide a rigorous framework to access tracer, intrinsic and interdiffusion coefficients in alloys with an arbitrary number of components. Utilization of the novel tracer-interdiffusion couple method allows for a high-throughput determination of composition-dependent tracer diffusion coefficients. A combination of these approaches provides a unique experimental toolbox to access diffusivities of elements which do not have suitable tracers. The 'pair-exchange diffusion model', which gives a consistent definition of diffusion matrices without specifying a reference element, is highlighted. Density-functional-theory-informed calculations of basic diffusion properties—as required for the generation of extensive mobility databases for technological applications—are discussed.

## Contents

1. INTRODUCTION .....	2
2. DIFFUSION IN MULTI-PRINCIPAL ELEMENT SYSTEMS: FEATURES AND CHALLENGES .....	3
3. TRACER DIFFUSION IN MULTI-PRINCIPAL ELEMENT ALLOYS .....	4
3.1. The role of crystalline lattice .....	6
3.2. The role of chemical and crystalline ordering .....	7
3.3. The role of interstitial alloying .....	8
4. ESTIMATION OF INTRINSIC AND TRACER DIFFUSION COEFFICIENTS FROM TERNARY AND MULTICOMPONENT DIFFUSION PROFILES .....	9
4.1. Ternary systems .....	9
4.2. Multicomponent systems .....	11
5. TRACER DIFFUSION IN CONCENTRATION GRADIENTS: AUGMENTED TRACER- INTERDIFFUSION COUPLE TECHNIQUE .....	13
6. AB INITIO SIMULATIONS OF DIFFUSION IN MULTI-COMPONENT SYSTEMS .....	14
6.1. Coarse-graining configurational space for defect diffusion energetics .....	16
6.2. Accurate vibrational free energies from machine learning potentials .....	17
6.3. Diffusion coefficients from kinetic Monte Carlo simulations .....	18
7. CALPHAD MODELING OF MULTI-COMPONENT DIFFUSION .....	19
8. SUMMARY AND CONCLUSIVE REMARKS .....	21

## 1. INTRODUCTION

Diffusion in multi-component systems, in particular those systems where a principal component cannot be identified, i.e. the 'multi-principal element systems', is an intriguing transport phenomenon with many fundamental features and both, experimental and theoretical challenges. Diffusion kinetics in general, and the analysis of diffusion-controlled processes in particular, are extremely important for both basic research and a further development towards industrial applications. Undoubtedly, diffusion in multi-principal element (usually five or more) alloys, often called as high-entropy alloys (HEAs), critically affects a number of crucial physical processes such as microstructural evolution, phase transitions, degradation and mechanical properties at elevated temperatures (1).

HEAs are often available as simple (random) solid solutions like, e.g., FCC CoCr-FeMnNi (2), BCC HfNbTaTiZr (3) or ZrNbTiVHf (4), and HCP HoDyYGDt (5) or  $\text{Al}_{15}\text{Hf}_{25}\text{Sc}_{10}\text{Ti}_{25}\text{Zr}_{25}$  (6) alloys, typically in a single phase state at higher temperatures. A relatively high thermal stability of such multi-principal element solid solutions advances them as ideal candidates for experimental and theoretical studies. Much of the fundamental diffusion-related research has been primarily driven by the concept of 'sluggish' diffusion in these random alloys (7). The hunt for 'sluggish diffusion' initiated plenty of studies since this concept was hypothesised without a thorough experimental verification. Since substitutional diffusion in typical metallic alloys is mediated by vacancies, one may modify the aim of the quest by asking whether the vacancy correlation factor—known to be just unity for self-diffusion in pure metals—is strongly reduced in HEAs. Such a hypothetical reduction would provide the fundamental reason for the sluggish diffusion phenomenon and thus clarify the strongly debated issue (8). However, although 'sluggish diffusion' was postulated as one of the core properties of HEAs (7), experimental studies have so far not supported this original concept (8, 9, 10).

---

HEA: high-entropy alloy

---

In this review, we aim first at a comparative analysis of experimental measurements of the diffusion kinetics in HEAs. We demonstrate how the specific sample composition along with the type of the crystalline lattice and potential ordering phenomena affect the diffusion transport. We show that diffusion can be both reduced as well as enhanced by the multi-element environment. Such measurements are in principle straightforward, though laborious, when utilizing the conventional radiotracer method, and we summarize the understanding gained from this method on various aspects of diffusion. The conventional diffusion couple method cannot be practiced in multi-component systems since the (one dimensional) diffusion paths cannot be forced to intersect in the (multi-dimensional) multi-component space. We demonstrate that the newly proposed pseudo-binary and pseudo-ternary methods circumvent this problem and thus can be applied in practice in these material systems. These methods are shown to be efficient experimental approaches that allow for a straightforward interpretation by producing physically reliable diffusion coefficients. The indirect estimation of tracer diffusion coefficients from these diffusion couple methods is also explained. Following the detailed experimental account, we focus on advances in theoretical investigations of diffusion in multi-principal element alloys via state-of-the-art *ab initio* simulations. A general framework for the consistent assessment of diffusion parameters is presented. Finally, recent advances in CALPHAD-type modeling of diffusion phenomena in multi-principal element systems are discussed. Thus, the whole spectrum of research is covered in this review, from accurate measurements of the diffusion parameters and the fundamental understanding of the diffusion mechanisms, alloy thermodynamics, and short- and long-range order to technological applications in the alloy development and predictions of life-time properties.

## 2. DIFFUSION IN MULTI-PRINCIPAL ELEMENT SYSTEMS: FEATURES AND CHALLENGES

Diffusion transport in solids is commonly measured by using either the tracer technique (usually radiotracer) or chemical- (or inter-) diffusion couples (11). Tracer diffusion experiments are typically performed on a homogeneous alloy of a given composition where the isotope transport is driven by entropy. For example, the self-diffusion measurements of Ni in a Ni-based alloy using the  $^{63}\text{Ni}$  tracer (12) correspond to a purely entropic driving force that governs the redistribution of the deposited marker atoms. On the other hand, solute (impurity) diffusion, e.g. of Cu in the Cu-free CoCrFeMnNi alloy using the  $^{65}\text{Cu}$  isotope (13), corresponds to chemical diffusion between the deposited film and the alloy. However, if the applied amount of the tracer atoms is vanishingly small, the measured 'chemical' interdiffusion coefficients coincide with the solute tracer diffusion coefficients in the solute-free alloy (14). In both cases, the chemical potential gradients that constitute the most general driving forces are reduced to the concentration gradients of the applied tracer atoms. Correspondingly, the tracer diffusion coefficients of any element can conveniently be measured in an alloy with an arbitrary number of alloying components. The recent results for FCC, BCC and HCP HEAs are critically reviewed in Sec. 3.

Chemical- or inter-diffusion is measured by bringing two different alloys in contact such that the atomic transport of the constituting elements is driven by the gradients of the chemical potentials. The interdiffusion coefficients can be straightforwardly determined for binary couples (in view of the Gibbs-Duhem relation, only one independent interdiffusion coefficient exists) along the whole interdiffusion path. In the case of ternary systems,

the whole  $2 \times 2$  matrix of interdiffusion coefficients can be determined for the composition corresponding to the intersection of two diffusion paths (14). For a long time, it was common textbook knowledge that the interdiffusion matrix cannot be determined for quaternary and higher-order systems, since it is experimentally impossible to enforce intersection of three (or more) independent interdiffusion paths at a single composition in a high-dimensional compositional space (14). Only very recently, new break-through approaches have been developed which seem to remove these long-standing limitations, as it will be discussed in Sec. 4.

Furthermore, using a very new approach of tracer diffusion in a concentration gradient (in fact, as usual, everything very new appears to be well forgotten old), reliable measurements of concentration-dependent tracer diffusion coefficients along the diffusion paths which develop in multi-component couples become feasible, see Sec. 5.

Does high configurational entropy (due to an increased number of elements in a multi-component alloy) retard inevitably substitutional diffusion? Self-diffusion in pure metals, known to be mediated by random motion of vacancies, is well understood (11). Already in random binary alloys—due to the different jump frequencies of different species—the vacancy jumps are not fully random forcing the corresponding vacancy correlation factor to be smaller than unity (15). Further, in a single-phase (solid solution) multi-principal element alloy, the vacancy jumps are inherently biased by the local energy barrier disorder (see Sec. 6). For example, relatively large fluctuations of the energy barriers (about 0.5 eV) were predicted for Cr and Fe atoms in the equiatomic CoCrFeMnNi alloy (16). Deep pits in the potential energy landscape for vacancy migration might be thought to retard vacancy migration. A percolation threshold of about 19.8% for the FCC lattice was predicted in a binary alloy with mobile and immobile components (15). Note that this value nearly coincides with the concentration of a single component in a typical five-element HEA. Thus, one may expect a strong dependence of the vacancy correlation factor on the alloy composition in such an alloy, if the frequency of vacancy exchanges with one element exceeds those for all other components by many orders of magnitude.

However, the percolation threshold almost disappears in a binary alloy if the difference of the energy barriers for slow and fast diffusing species,  $\Delta E_m$ , is relatively small,  $\Delta E_m \leq 5kT$  (17). Taking a typical diffusion temperature of 1300 K, one comes to the conclusion that the percolation concept would lose its importance for a typical random alloy, if the difference of the energy barriers is  $\Delta E_m \leq 0.6$  eV. Otherwise one may expect a certain retardation of the atomic transport in a HEA due to the strong correlations of successive vacancy jumps.

In the next sections, we will analyze whether these predictions are relevant for the HEAs investigated so far.

### 3. TRACER DIFFUSION IN MULTI-PRINCIPAL ELEMENT ALLOYS

Tracer diffusion measurements (with suitable radioactive or highly enriched natural isotopes) is one of the most powerful techniques to determine the tracer diffusion coefficients,  $D_i^*$ , (directly related to the atomic mobilities,  $M_i$ ) of an element  $i$  in a given alloy of a certain composition (11). Typically, a chemically homogeneous alloy is used and the determination of individual tracer diffusion coefficients of all constituting elements in a multi-component alloy for a reasonably large number of compositions in an extended temperature interval does represent a laborious and time-consuming task. This is why such measurements have been so far typically limited to pure metals (self-diffusion for a limited number of met-

## Tracer diffusion in high-entropy alloys and impact of

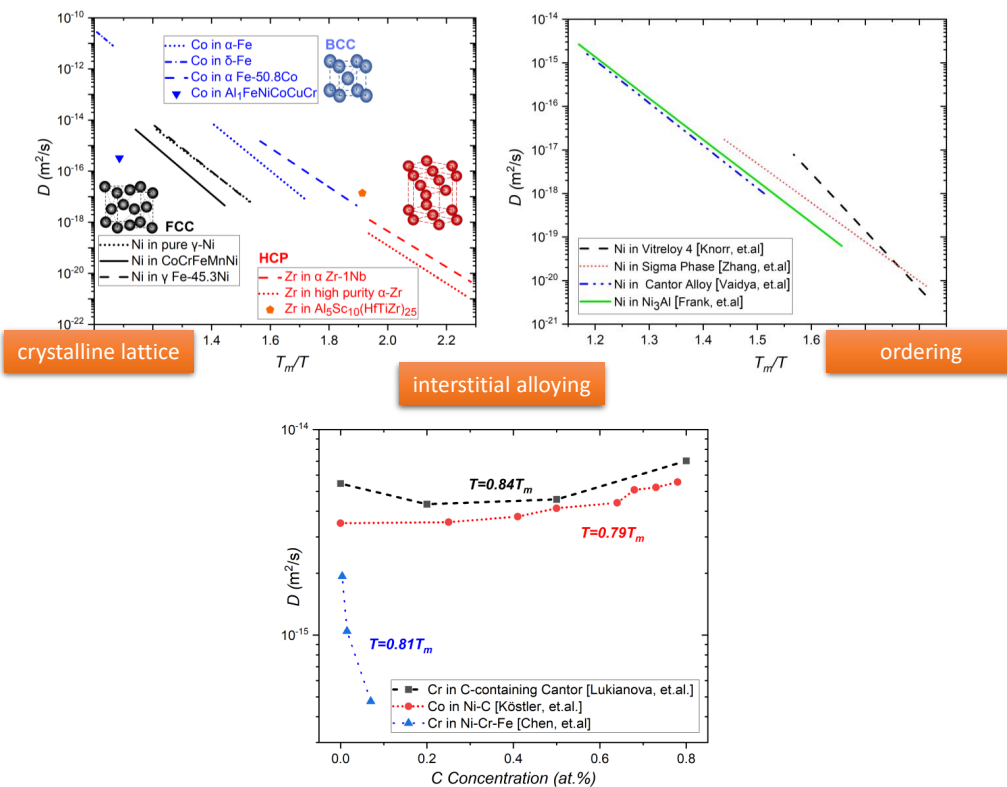


**Figure 1**

(top-left) Tracer diffusion coefficients,  $D^*$ , of selected constituting elements in FCC (Ni, black lines), BCC (Co, blue lines) and HCP (Zr, red lines) systems as function of the inverse homologous temperature,  $T_m/T$ . The corresponding diffusion rates are compared for pure elements (Ni (18),  $\alpha$ - and  $\delta$ -Fe (19), and  $\alpha$ -Zr (20)), binary ( $\gamma$ -Fe-Ni (21),  $\alpha$ -Fe-Co (22), and  $\alpha$ -Zr-Nb (20)) and high-entropy (CoCrFeMnNi (13),  $\text{Al}_x\text{FeNiCoCuCr}$  (23) and  $\text{Al}_5\text{Hf}_{25}\text{Sc}_{20}\text{Ti}_{25}\text{Zr}_{25}$  (24)) alloys.  $T_m$  is the melting point of the corresponding compounds.

(top-right) Ni tracer diffusion coefficients  $D^*$  plotted as a function of homologous temperature  $T_m/T$  for different multicomponent systems with varying crystal structures – FCC CoCrFeMnNi HEA (13), Cr-rich  $\sigma$ -phase (25), Ni<sub>3</sub>Al (26) and bulk metallic glass Vitreloy 4 (27).

(bottom) The impact of interstitial carbon addition to various FCC systems on tracer diffusion of Co in binary Ni-C (28) and Cr in quaternary NiCrFe-C (29) and senary CoCrFeMnNi-C (30) alloys. The diffusivities are compared at about  $0.8T_m$ .

als only, e.g. Ba, has not yet been measured), binary and seldom ternary alloys (31). Multi-principal element alloys with five and more elements clearly pose a challenge to the experimental capabilities.

We summarize and compare in the following sections the measured tracer diffusion coefficients available so far for a collection of near equiatomic HEAs possessing different compositions, lattice structures, chemical and lattice ordering to demonstrate their respective roles in diffusion.

### 3.1. The role of crystalline lattice

Most of the tracer diffusion studies on HEAs reported so far have been performed on FCC systems (32, 33, 12, 13), with only a very few studies on BCC (23) or HCP (24) systems. It is still an open question whether the knowledge gained for FCC alloys can be transferred to other crystalline symmetries, since diffusion in FCC HEAs has been measured in extended temperature intervals while that in BCC or HCP alloys only at representative temperatures, Fig. 1, top-left panel.

In Fig. 1, top-left panel, the tracer diffusion coefficients of representative constituent elements in HEAs of different crystalline symmetries are compared using the inverse homologous scale,  $T_m/T$ . Here  $T_m$  is the melting point of the corresponding alloy taken as the temperature corresponding to the maximum of the heat release during calorimetric measurements. The diffusion coefficients in different crystalline lattices are distinguished by colors and self-diffusivities in pure metals, selected binary alloys and HEAs are compared to figure out the heavily discussed impact of the configurational entropy on the diffusion rates of substitutional elements.

What is immediately evident from Fig. 1, top-left panel, is that at the same homologous temperature the self-diffusivities in FCC systems are significantly smaller as compared to those in the BCC systems which exhibit obviously more open structures that facilitate vacancy-mediated diffusion.

Self-diffusion in the HCP systems is most intriguing. Whereas the reduced (i.e., scaled on the melting point) activation energies of self-diffusion in FCC and HCP pure metals are similar (the well-known textbook knowledge (11)), Zr diffusion in the HCP HEA is significantly enhanced with respect to that in unary HCP metals, whereas some retardation of diffusion is observed in FCC HEA. In fact, the HCP systems show a very clear trend towards 'anti-sluggishness' of diffusion induced by the multi-component environment when compared on the homologous temperature scale. It has been reported that even minute amounts of impurities (such as Fe or Co) present in technically pure  $\alpha$ -Ti or  $\alpha$ -Zr enhance the self-diffusion rates, especially at low temperatures (34). The most surprising finding, however, is that Zr diffuses significantly faster in the non-equiatomic HCP  $\text{Al}_{15}\text{Hf}_{25}\text{Sc}_{10}\text{Ti}_{25}\text{Zr}_{25}$  HEA than in unary Zr or binary Zr-Nb by orders of magnitude, Fig. 1, top-left panel. The reasons of such an enhancement are still to be elucidated.

Considering the FCC systems (black lines), self-diffusion of Ni in the CoCrFeMnNi Cantor HEA (33, 13) is slower than that in the unary Ni (18) and binary Fe-45.3Ni (21), suggesting a certain sluggishness of diffusion. The same sluggishness, however, does not seem to be true for the HCP systems.

Looking at the BCC systems, reported (23) Co diffusion in the BCC AlCoCrFeNi is significantly slower as compared to Co diffusion in paramagnetic  $\alpha$ - or  $\delta$ -Fe (19) with the BCC lattice. The Co diffusion rate in nearly equiatomic BCC Fe-Co alloy is enhanced

with respect to that in pure Fe, Fig. 1, top-left panel. One may anticipate a significant retardation of substitutional diffusion in BCC multi-principal element alloys. However, the AlCoCrFeNi alloy features a two-phase, FCC + BCC/B2 microstructure (35), and the diffusivities reported in Ref. (23) might be representative for the FCC component. Tracer diffusion measurements in single-phase BCC HEAs are required to shed light on the retardation/enhancement of diffusion induced by the multi-principal element environment in the BCC lattice.

Following the arguments of Tsai et al. (36), one may suggest that diffusing vacancies experience different local mismatches between neighbouring atoms and differences in bond strengths. Thus, fluctuations of lattice potential energies are expected which can affect vacancy migration via the multi-component matrix. An increased number of alloying components might increase these local fluctuations. Loosely speaking, one may hypothesise a reduction of atomic mobility as induced by increased configurational entropy. However, it is clearly not just increased configurational entropy which retards diffusion, since chemical disordering (associated with an increase of the configurational entropy) enhances typically diffusion rates, at least in binary ordered alloys (37).

For further analysis, one needs to quantify the distortions induced by multi-component environments in HEAs. The normalized potential energy fluctuations,  $x_p$ , were proposed (38, 10) to be determined by the sum of elastic distortions,  $x_e$ , and chemical interactions,  $x_{ch}$ ,

$$x_p = x_e + x_{ch} = 4.12\delta\sqrt{\frac{\bar{K}\bar{V}}{k_B T}} + 2\left(\frac{\sqrt{\sum_i \sum_{j,j \neq i} (\Delta H_{ij}^{\text{mix}} - \bar{H})^2}}{k_B T}\right)^{1/2} \quad 1.$$

Here  $\delta = \sqrt{\sum_i (1 - \frac{r_i}{\bar{r}})^2}$  is the atomic distortion in equiatomic alloy with  $r_i$  and  $\bar{r}$  being the atomic radius of element  $i$  and the mean atomic radius of all elements in the alloy.  $\bar{K}$  and  $\bar{V}$  are the averaged bulk compressibility and atomic volume, respectively.  $\Delta H_{ij}^{\text{mix}}$  and  $\bar{H}$  are the binary pair enthalpy of mixing of elements  $i$  and  $j$  and its averaged value for the alloy, respectively. In non-equiatomic alloys, all averaged values are taken as composition-weighted ones.

A simple comparison of the atomic radius mismatches for the HEAs in question ( $\delta = 1.6\%$ ,  $3.8\%$  and  $7.2\%$  for FCC, BCC and HCP alloys, respectively) suggests a strong impact of the elastic distortions on 'sluggishness' of diffusion in HEAs. In FCC CoCrFeMnNi alloys with a relatively small elastic mismatch, diffusion retardation due to an increase of the number of components is observed. On the other hand, an enhancement of the diffusivity is seen in the HCP AlHfScTiZr systems. This behavior suggests a strong impact of the elastic distortions on substitutional diffusion in multi-component alloys. Is this a 'pressure-like' enthalpic term (i.e.,  $\exp(\sigma\Omega/k_B T)$  with  $\sigma$  and  $\Omega$  being local stress and activation volume of diffusion) or increased vibrational entropy at a higher level of elastic distortions? This question has to be elucidated. An absence of a clear correlation of the total  $x_p = x_e + x_{ch}$  value with the diffusion rate in a wide spectrum of FCC alloys has already been stated (10). We conclude that increased potential energy fluctuations do not inevitably induce retardation of the diffusion rates.

### 3.2. The role of chemical and crystalline ordering

In Fig. 1, top-right panel, the Ni tracer diffusion coefficients in the disordered FCC CoCrFeMnNi Cantor alloy (33, 13), the  $\sigma$  phase of the  $\text{Co}_{17}\text{Cr}_{46}\text{Fe}_{16.3}\text{Mn}_{15.2}\text{Ni}_{5.5}$  alloy (25), the

ordered  $L1_2$  Ni<sub>3</sub>Al (26), and bulk metallic glass Vitreloy 4 Zr<sub>46.75</sub>Ti<sub>8.25</sub>Cu<sub>7.5</sub>Ni<sub>10</sub>Be<sub>27.5</sub> (27) are compared using the homologous temperature scale. It has to be noted that the comparison is made for the homologous temperatures where tracer diffusion coefficients were measured in the respective works.

Comparing Ni self-diffusion in the CoCrFeMnNi multi-principal element alloy with simple FCC random solid solution with the ordered  $L1_2$  Ni<sub>3</sub>Al intermetallic compound with FCC-derived structure, it can be clearly observed that Ni diffuses in Ni<sub>3</sub>Al almost at the same rates as in the Cantor CoCrFeMnNi alloy. The Ni diffusion mechanism in  $L1_2$ -ordered Ni<sub>3</sub>Al is well-known (37) and it corresponds to the sublattice diffusion mechanism. In Ni<sub>3</sub>Al, vacancies are dominantly available on the Ni sublattice with the coordination number of 8 and the Ni atoms diffuse via nearest-neighbor jumps over the Ni sublattice (37). One may speculate that the local chemical disorder in the CoCrFeMnNi alloy with the given spectrum of the migration barriers for Ni atoms in particular, is somehow equivalent to the decrease of the coordination number of Ni atoms from 12 to 8. In other words, a fraction of the crystallographic sites of the FCC lattice might be not accessible for diffusing Ni atoms due to relatively large associated migration barriers in the CoCrFeMnNi alloy.

The  $\sigma$  phase that is generally observed in the Cantor and pseudo-Cantor systems at certain temperature ranges displays an enhanced Ni diffusivity as compared to the cubic systems. The crystalline lattice of the  $\sigma$ -phase features five distinct sublattices with different occupation probabilities for different elements (25). The relative enhancement of Ni diffusion in Cr-rich  $\sigma$ -phase with respect to equiatomic CoCrFeMnNi reference alloy has been explained by an increased vacancy concentration and decreased migration barriers due to the addition of Cr atoms instead of Ni ones (25). Nevertheless, a DFT-informed input from theoretical analysis of diffusion in the  $\sigma$ -phase is missing so far.

A bulk metallic glass, e.g. Vitreloy 4, is characterized by both chemical and crystalline disorder in view of the absence of the translational order. Below about  $0.6T_m$ , Fig. 1, top-right panel, Ni diffusion in the Zr<sub>46.8</sub>Be<sub>27.5</sub>Ti<sub>8.2</sub>Cu<sub>7.5</sub>Ni<sub>10</sub> (Vitreloy 4) metallic glass becomes retarded and slowest among the given systems. At higher homologous temperatures, diffusion in the Vitreloy 4 is even faster than in crystalline lattices, probably due to fundamentally different diffusion mechanisms. Note that a collective, string-like motion of groups of atoms has been suggested for diffusion in bulk metallic glasses (39), whereas substitutional diffusion in crystalline lattices is mediated by vacancies.

### 3.3. The role of interstitial alloying

The impact of interstitial alloying, in particular C atoms, on the mobility of substitutional atoms has been recently investigated in details (30). We compare in Fig. 1 (bottom panel) the substitutional diffusion in binary Ni-C (Co diffusion) (28), quaternary Ni-Cr-Fe-C (Cr diffusion) (29), and senary CoCrFeMnNi-C alloys (Cr diffusion) (30) at about  $0.8T_m$ . Similar trends are generally seen for all investigated systems. The addition of C decreases first the substitutional diffusion rates, i.e. the diffusion coefficients drop slightly from the C-free alloy to alloys with 0.2% C (the effect is stronger in Ni-Cr-Fe-C system). A further increase of the C concentration enhances the substitutional diffusion rates, which is explained by the increased vacancy concentration due to the induced lattice distortions (30). Carbon atoms occupy interstitial sites with chemically different environments that induces local strains and might be responsible for the experimentally-observed substitutional diffusion enhancement.



## 4. ESTIMATION OF INTRINSIC AND TRACER DIFFUSION COEFFICIENTS FROM TERNARY AND MULTICOMPONENT DIFFUSION PROFILES

The radioisotope method demonstrated in the previous section becomes sometimes almost unfeasible for the direct estimation of tracer diffusion coefficients of several components in ternary and multicomponent systems because of short half-life (e.g.,  $^{32}\text{Si}$ ) or very costly (e.g.,  $^{26}\text{Al}$ ) radioisotopes. The diffusion couple technique does not have these restrictions. However, this method had faced an unsolved challenge for estimating diffusion coefficients experimentally in a multicomponent system. The problems have been solved up to a certain extent following the new methods recently proposed. Even the tracer diffusion coefficients of all the components can be estimated utilizing the thermodynamic parameters. These are first explained in ternary systems and then extended to the higher-order systems. A few ideas, which were not practiced before, are also proposed along with the methods already established.

The interdiffusion coefficients ( $D_{ij}^n$ ), interdiffusion flux ( $\tilde{J}_i$ ) and composition gradient ( $\frac{\partial N_j}{\partial x}$ ) of component  $i$  in an  $n$  component system considering constant molar volume ( $V_m$ ) are related by (14, 40)

$$\tilde{J}_i = -\frac{1}{V_m} \sum_{j=1}^{n-1} \tilde{D}_{ij}^n \frac{\partial N_j}{\partial x} \quad 2.$$

The interdiffusion flux of components can be calculated directly from the composition profiles (14). We need to estimate  $(n-1)^2$  independent interdiffusion coefficients in an  $n$  component system by intersecting  $(n-1)$  diffusion paths in a multicomponent space. This is easy in a ternary system (to force two 1D diffusion paths to intersect on a 2D surface) but almost impossible in a system with more than three components (40). The  $n(n-1)$  independent intrinsic diffusion coefficients are related to the interdiffusion coefficients by (40)

$$\tilde{D}_{ij}^n = D_{ij}^n - N_i \sum_{k=1}^n D_{kj}^n \quad 3.$$

Based on Manning's formalism, the intrinsic diffusion coefficients ( $D_{ij}^n$ ) are related to the tracer diffusion coefficients,  $D_i^*$ , and thermodynamic factor,  $\theta_{ij}^n$ , by (41)

$$D_{ij}^n = \frac{N_i}{N_j} D_i^* \theta_{ij}^n + \xi N_i D_i^* \sum_{k=1}^{n-1} \frac{N_k}{N_j} (D_k^* - D_n^*) \theta_{kj}^n \quad 4.$$

where  $\xi = \frac{2}{S_o \sum_{j=1}^n N_j D_j^*}$  and  $S_o$  is the structure factor (41, 42).

Darken (43) and Le Claire (44) neglected the cross phenomenological terms of the Onsager formalism (45, 46) to relate  $D_{ij}^n$  with  $D_i^*$  by the first term only. The second term of Manning's formalism is related to the vacancy wind effect (41, 42), which may influence certain intrinsic diffusion coefficients strongly (47).

### 4.1. Ternary systems

All types of diffusion coefficients could be estimated following the diffusion couple method only in binary systems, which are described elsewhere (14). Following Eq. 2, we need to estimate two main ( $\tilde{D}_{22}^1, \tilde{D}_{33}^1$ ) and two cross ( $\tilde{D}_{23}^1, \tilde{D}_{32}^1$ ) interdiffusion coefficients in a ternary system considering, e.g., component 1 as the dependent variable (48). We can estimate these parameters at the composition corresponding to the intersection of two diffusion

couples. The interdiffusion coefficients are kind of composition-average of intrinsic diffusion coefficients, which are related by Eq. 3. However, the six intrinsic diffusion coefficients ( $D_{12}^1, D_{13}^1, D_{22}^1, D_{23}^1, D_{32}^1, D_{33}^1$ ) could not be estimated in a ternary system following the Kirkendall marker experiments. One can easily intersect two diffusion profiles in a ternary system for the calculation of four interdiffusion coefficients. However, it is almost impossible to predict the end-member compositions *a priori* to find the Kirkendall marker plane at the composition of intersection in both the diffusion couples (40) to solve six equations for the estimation of six intrinsic diffusion coefficients.

Kirkaldy and Lane (49) proposed the method of estimating first the tracer diffusion coefficients at the composition of intersection in a ternary system, which then facilitates the calculation of intrinsic diffusion coefficients as well. We can substitute Eq. 4 in Eq. 3 to express the interdiffusion coefficients with respect to the tracer diffusion coefficients and the thermodynamic factors. They proposed the relations with respect to chemical potential gradients and van Loo et al. (50) proposed to write these equations with respect to the thermodynamic factors, which are materials constants. With interdiffusion coefficients estimated from the composition profiles directly at the composition of intersection and known thermodynamic factors, one can determine the tracer diffusion coefficients. Once the tracer diffusion coefficients are estimated, the intrinsic diffusion coefficients can be calculated utilizing Eq. 4.

---

**PB:** pseudo-binary

**PT:** pseudo-ternary

---

There are certain advantages of practicing the recently proposed pseudo-binary (PB) diffusion couple technique over the method described above (51, 52, 53, 8, 54). In this, the composition of one component (let us say 3) is kept the same in the two end-members of a diffusion couple. When this component remains constant in the interdiffusion zone as well, such that only two components contribute to the diffusion profile, we can estimate the composition dependent PB interdiffusion coefficient ( $\tilde{D}_{PB}$ ) over the whole composition range from a single diffusion couple (similar to the binary system) from (47)

$$\tilde{J}_i V_m = -\tilde{D}_{PB} \frac{\partial N_i}{\partial x} \quad 5a.$$

As demonstrated extensively (47, 52, 53) two intrinsic diffusion coefficients,  $D_{22}^1$  and  $D_{11}^2$ , can be estimated directly from the composition profile at the Kirkendall marker plane following an augmented Darken-Manning approach, which are related by

$$\tilde{D}_{PB} = M_1^B D_{22}^1 + M_2^B D_{11}^2 \quad 5b.$$

where  $M_i^B = \frac{N_i}{N_1 + N_2}$  is the modified composition relevant for the PB couple in a solid solution. The modified composition should be written differently in an intermetallic compound considering how the components occupy different sublattices (55, 56, 57). Following, the tracer diffusion coefficients can be calculated from (47)

$$D_{11}^2 = D_1^* [\theta_{11}^2 + M_1^B \xi_{PB} (D_1^* \theta_{11}^2 - D_2^* \theta_{22}^1)] \quad 6a.$$

$$D_{22}^1 = D_2^* [\theta_{22}^1 - M_2^B \xi_{PB} (D_1^* \theta_{11}^2 - D_2^* \theta_{22}^1)] \quad 6b.$$

where  $\xi_{PB} = \frac{2}{S_o \sum_{j=1}^2 M_j^B D_j^*}$  (47) and  $S_o$  is the structure factor (42).

One can also estimate the tracer diffusion coefficients at the intersecting composition of ternary and pseudo-binary diffusion paths (see Fig. 2). Two independent interdiffusion fluxes of a ternary diffusion couple can be expressed with the tracer diffusion coefficients

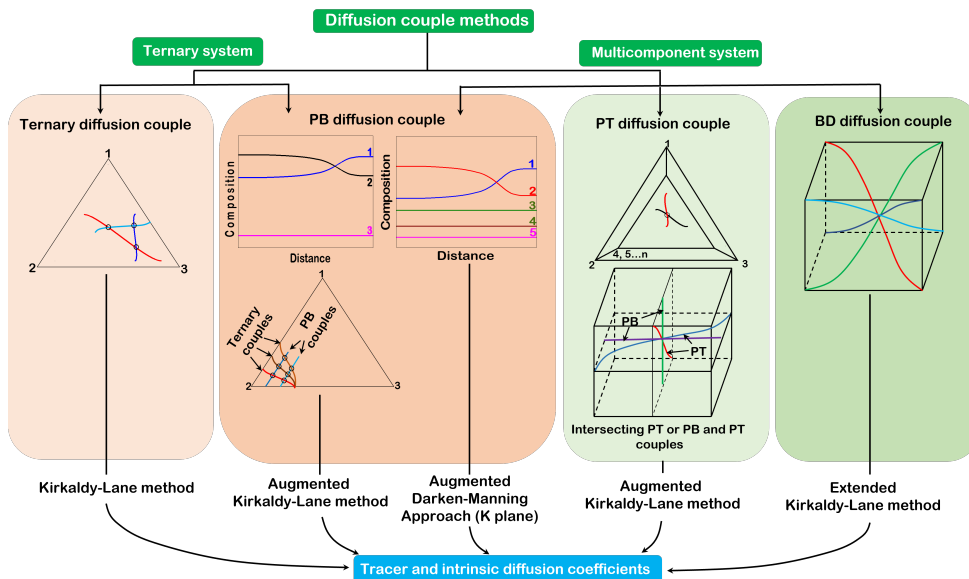


Figure 2

Diffusion couple methods in multicomponent systems

and thermodynamic parameters by replacing Eq. 3 and 4 in Eq. 2. The interdiffusion flux of PB couple can be expressed similarly by substituting 6a, 6b and 5b in 5a. The tracer diffusion coefficients can be then calculated utilizing the thermodynamic parameters at the composition of intersection. One can design the experiments such that several ternary diffusion paths intersect one PB diffusion path for estimation of the tracer diffusion coefficients systematically with the change in composition along the diffusion (composition) path of a PB couple (see Fig. 2). Such systematic estimation is difficult by intersecting only ternary diffusion paths because of unknown serpentine nature of the ternary diffusion paths *a priori*.

## 4.2. Multicomponent systems

The estimation of diffusion coefficients in a multicomponent system is almost impossible by intersecting the diffusion paths exactly in a multicomponent space (58). Morral (59) proposed the concept of the body diagonal diffusion couple method in a small composition range of constant diffusivities with the possibilities of  $(n-1)$  diffusion paths passing closely with different distances (instead of intersecting) for estimation of  $(n-1)^2$  interdiffusion coefficients (60). One may rather calculate tracer diffusion coefficients by extending the Kirkaldy-Lane method from only two diffusion couples with closest paths. Equations 4 and 3 can be substituted in Eq. 2 to express the  $2(n-1)$  interdiffusion fluxes with respect to the tracer diffusion coefficients, known thermodynamic factors and composition gradients. A least square method can then be used to calculate the  $n$  tracer diffusion coefficients. Following, one can calculate the intrinsic diffusion coefficients from Eq. 4 and then the interdiffusion coefficients from Eq. 3 (47).

As already explained, one can practice the PB diffusion couple in a multicomponent system by producing the diffusion couples such that only two components develop the dif-

fusion profiles keeping all other components as the constant (47, 52, 53). In an unpublished research, we have produced such ideal and near-ideal PB diffusion couples up to six or seven components. However, this method helps to estimate only the main diffusion coefficients. Therefore, the concept of pseudo-ternary (PT) diffusion couple method is established following which a set of both main and cross-diffusion coefficients can be estimated (47, 61). In this only three components develop the diffusion profiles keeping the other components constant. This restricts the diffusion paths on a two-dimensional plane similar to the ternary system and makes it possible to intersect the diffusion paths exactly. In such a situation, considering only components 1, 2 and 3 develop the diffusion profiles keeping all other components 4- $n$  as the constant, four interdiffusion coefficients ( $\tilde{D}_{22}^1, \tilde{D}_{33}^1, \tilde{D}_{23}^1, \tilde{D}_{32}^1$ ) are estimated (similar to a ternary system). These are related to six intrinsic diffusion coefficients ( $D_{12}^1, D_{22}^1, D_{32}^1, D_{13}^1, D_{23}^1, D_{33}^1$ ) by (47)

$$\tilde{D}_{ij}^1 = D_{ij}^1 - M_i^T (D_{1j}^1 + D_{2j}^1 + D_{3j}^1) \quad 7a.$$

where  $M_i^T = \frac{N_i}{N_1+N_2+N_3}$ . This normalization of composition is different in the intermetallic compound as explained in (55). However, similar to the ternary system, these are very difficult to estimate following the Kirkendall marker experiments. To circumvent this problem, the augmented Kirkaldy and Lane method is developed for the PT couple (47). The intrinsic and tracer diffusion coefficients in a PT diffusion couple are related by (47)

$$D_{ij}^1 = \frac{M_i^T}{M_j^T} D_i^* \theta_{ij}^1 (1 + W_{ij}) \quad 7b.$$

where  $1 + W_{ij} = 1 + \frac{2(M_1^T D_1^* \theta_{ij}^1 + M_2^T D_2^* \theta_{ij}^2 + M_3^T D_3^* \theta_{ij}^3)}{S_o(M_1^T D_1^* + M_2^T D_2^* + M_3^T D_3^*)}$  is the vacancy wind effect.

Therefore, one can estimate three tracer diffusion coefficients of the diffusing components by substituting Eq. 7b in 7a and calculate the tracer diffusion coefficients from the estimated interdiffusion coefficients and known thermodynamic parameters. We have found an excellent match in the estimated data following this method and the radiotracer technique in NiCoFeCr system (47, 53). The tracer diffusion coefficients of only three and two components can be estimated from one type of PT and PB couple, respectively. Therefore, if possible, one can consider a set of intersecting PB and PT couples for estimation of the tracer diffusion coefficients of all the components (see Fig. 2). This is found to be feasible in NiCoFeCr system with possibilities to extend in many other systems. Following, one can estimate the intrinsic and interdiffusion coefficients of all the components (47).

Based on our analysis, an undetectable non-ideality in the diffusion profiles of the components (if present) which are supposed to remain constant, do not induce mentionable errors in calculations and such can be treated as ideal PB or PT diffusion couples. Sometimes, these components may develop detectable but very minor diffusion profiles instead of remaining constant. By forcing the PB condition, one may still be able to calculate the PB diffusion coefficients with very minor errors. An extensive analysis is still required analyzing errors in the calculations depending on the extent of the non-ideality in these types of couples. The error analysis is also required in body-diagonal couples since the diffusion profiles do not intersect inherently that might induce an unknown error.

To summarize, a combination of different diffusion couple methods can be used first to estimate the tracer diffusion coefficients of different components and then calculate the intrinsic and interdiffusion coefficients. We are highlighting that this method by-passes

the limitations imposed on the radiotracer methods due to the absence of easy-to-handle radioisotopes in several technologically important cases (e.g., Al or Si).

## 5. TRACER DIFFUSION IN CONCENTRATION GRADIENTS: AUGMENTED TRACER-INTERDIFFUSION COUPLE TECHNIQUE

In his PhD thesis in 1950s, Manning proposed to combine the tracer and chemical diffusion measurements in a single experiment and address thermodynamic properties of the alloy (62). The corresponding experiments, carried out on binary Ag-Cd (62) and Ag-Au (63), were focused on the separation of the effects stemming from the vacancy flux and thermodynamic factors.

Almost about 60 years later, Murch and Belova with co-authors (64, 65) re-analysed the original experiments and developed a framework for rigorous determination of the concentration-dependent tracer diffusion coefficients along the whole diffusion path which is produced in a binary couple. The proposed experimental approach was then further elaborated by Gaertner et al. (66) and applied for diffusion measurements in a multi-component  $\text{Co}_{15}\text{Cr}_{20}\text{Fe}_{20}\text{Mn}_{20}\text{Ni}_{25}/\text{Co}_{25}\text{Cr}_{20}\text{Fe}_{20}\text{Mn}_{20}\text{Ni}_{15}$  couple. Recently, the augmented tracer-interdiffusion couple approach has been successfully utilized for assessment of concentration-dependent Ga tracer diffusion coefficients in binary Fe-Ga couples via measuring tracer diffusion of the  $^{59}\text{Fe}$  isotope in the corresponding concentration gradients (67).

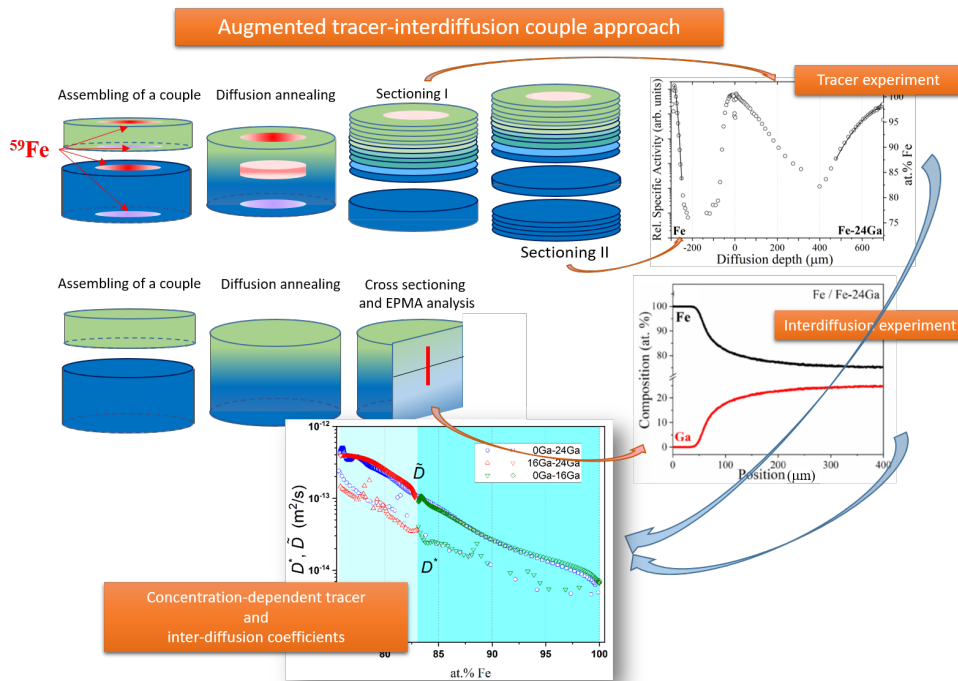


**Figure 3**

A scheme of augmented tracer-interdiffusion method in application to the Fe-Ga system. For further details see the work of Muralikrishna et al. (67).

The augmented tracer-interdiffusion couple approach is sketched in Fig. 3. A tracer isotope (in the particular case, the  $^{59}\text{Fe}$  radioisotope (67)) is applied to both opposite surfaces of each half of the diffusion couple before the samples are brought in contact. After annealing, the diffusion couple is sectioned through and the *tracer concentration profiles* are determined (upper panel). An identical couple is cross-sectioned and the *element concentration profiles* are measured using an electron micro-probe analysis (medium panel). Having determined both tracer and chemical concentration profiles, the tracer diffusion coefficient is determined as a function of the composition (bottom panel). The tracer diffusion coefficients are independently measured in two end-members with the homogeneous compositions, too. A consistency of the whole data set underlines the correctness of the approach (66, 67). In the case of binary couple, the interdiffusion coefficient can be determined as well, Fig. 3, bottom panel. If the approach is applied to a pseudo-binary couple in a multi-component alloy, the tracer diffusion coefficients and the PB interdiffusion coefficients can be determined. In the case of an arbitrary multi-component couple, only tracer diffusion coefficients (as a function of the concentration along the developed diffusion path) will be determined (66).

The augmented tracer-interdiffusion couple method allows a consistent determination of the concentration-dependent tracer diffusion coefficients in general diffusion couples along whole interdiffusion paths in the multi-component alloys (including the end-members). The independent tracer diffusion measurements in the unaffected end-members facilitate to overcome the limitations related to the common difficulties with correct determination of the concentration gradients and integration of the concentration profiles near the end-member compositions.

Combination of pseudo-binary or pseudo-ternary couples (see Sec. 4) with the tracer-interdiffusion method offers unprecedented advantages to access the tracer and interdiffusion (as well as intrinsic) coefficients in the same couples. In the case of existing thermodynamic description, the tracer diffusion coefficients of elements for which no suitable radioisotopes exist could be determined. The PB and PT approaches allow independent determination of the tracer diffusion coefficients that again provides access to atomic mobilities of the chemical elements with no suitable radioisotopes (such as, e.g., Al or Ga in Ref. (67)).

## 6. AB INITIO SIMULATIONS OF DIFFUSION IN MULTI-COMPONENT SYSTEMS

As discussed in previous sections, various diffusion coefficients in HEAs are experimentally accessible via the diffusion couple or radiotracer techniques, including the newly-developed tracer-interdiffusion couple approach. The composition- and/or temperature-dependent diffusion rates can be utilized to extract diffusion parameters such as the activation energies and the pre-factors. This information, being prone to large uncertainties when the measurements are done in experimentally-accessible temperature intervals, however, provides only limited physical insight into the related diffusion mechanisms behind the observed phenomena. Very special tracer experiments focused, e.g., on pressure dependence or isotope effect (11) are required. Theoretical predictions, especially based on state-of-the-art *ab initio* density-functional-theory (DFT) simulations, provide an alternative approach to obtain the diffusion rates and diffusion properties. An attractive bonus offered by such simulations beyond the mere calculated diffusion data is a thorough microscopic understanding of the observed phenomena. Moreover, the DFT-informed calculations may provide a unique access

to the diffusion parameters in the metastable phases, heavily required for CALPHAD-like modelling (see Sec. 7) but inaccessible for the experiments.

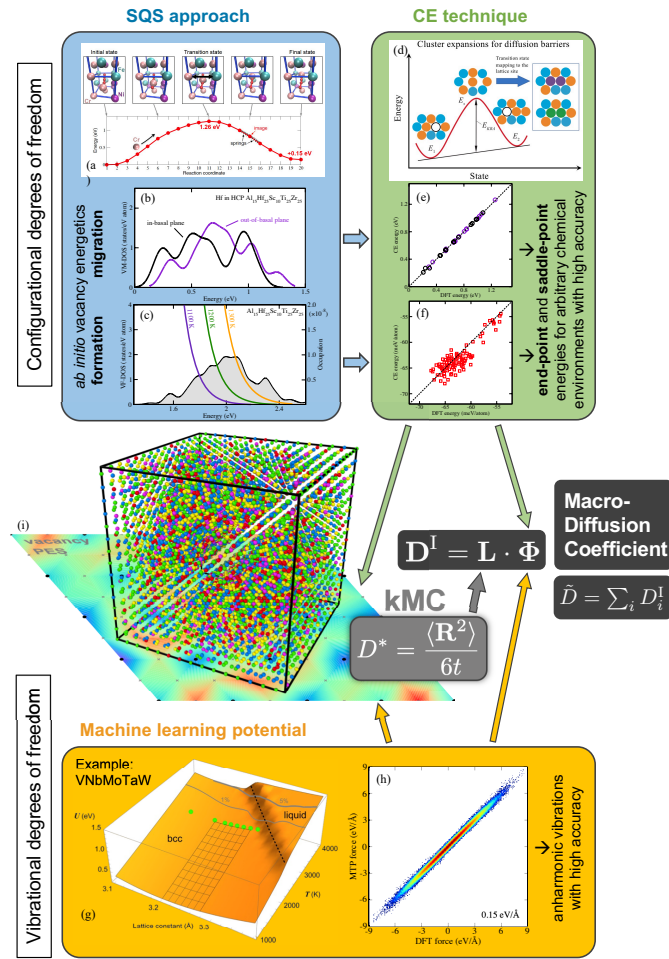


Figure 4

*Ab initio* simulations of diffusion in HEAs.

Nowadays, *ab initio* prediction of diffusivities and related properties in low-order systems, e.g., pure metals or binary alloys in the dilute limit, has become commonplace. For self- and solute-diffusion in pure metals and dilute alloys, excellent agreement with high temperature experimental data can be achieved provided that the relevant thermal excitation effects are taken into account since the configurational degrees of freedom are very limited. Going beyond the well-established quasiharmonic approximation, accurate and efficient *ab initio* methodologies for explicit anharmonicity have acquired maturity and have shown great success in recent years. However, the *ab initio* computational framework utilized for diffusion in pure metals and dilute alloys breaks down for concentrated multicomponent alloys due to the explosive configurational space. In such alloys, the energetics relevant

---

**DFT:** density functional theory

**SQS:** special quasirandom structure

**DOS:** density of states

**NEB:** nudged elastic band

---

for diffusion simulations, e.g., formation and migration energies of vacancies or interstitial defects, becomes very sensitive to the chemical environment. The chemical environment may also have a strong impact on the vibrational degrees of freedom, further increasing the challenges in the exploration of diffusion in concentrated multicomponent alloys. In the following subsections, we present recent methodological developments that address the diffusion energetics related to both configurational and vibrational degrees of freedom in multicomponent systems. We also introduce approaches to extract various diffusion coefficients. Finally, possible future developments will be suggested and discussed.

### 6.1. Coarse-graining configurational space for defect diffusion energetics

From the atomistic perspective, we focus in this review article mainly on substitutional (vacancy-mediated) and interstitial (impurity atoms) bulk diffusion as these diffusion mechanisms are generally the dominant ones. Among the key quantities that are necessary to calculate the diffusion rates and to understand the involved physics are the defect diffusion energies, i.e., formation and migration energies of the defects. The formation energies in particular determine the concentration/solubility of the defects with which the diffusion rates scale. In general, it has been concluded that the chemical configuration in the vicinity of a defect has a strong impact on its formation and migration energies. The resulting effective energetics must be extracted based on a statistical analysis with the knowledge of the distribution of individual defect energy states, i.e., the 'density of defect states' (defect-DOS). Unlike in pure metals or dilute alloys where defects are associated with a small number of local atomic environments, *ab initio* modeling of defect properties in concentrated multicomponent alloys faces significant challenges as the number of chemical environments combinatorially explodes with the number of components. In order to achieve sufficient statistics for sampling the defect-DOS, different coarse-graining approaches can be applied. We will mainly discuss here the *ab initio* DFT-based approaches followed by a brief overview of the other methods.

**Special quasirandom structures approach.** To fully retain DFT accuracy, the most straightforward approach is, in principle, to perform explicit DFT calculations for structures/supercells containing defects for all different chemical arrangements. The immense number of configurations prohibits such a brute-force exploration; e.g., in a 5-component FCC HEA there are  $5^{12} \approx 2 \times 10^8$  configurations for the nearest neighbor shell of a vacancy (taking the symmetry into account may reduce this number slightly). As HEAs generally exhibit single-phase random solid solutions at compositions and temperatures where diffusion is experimentally measured, the widely-used 'special quasirandom structure' (SQS) approach (68) is ideal to mimic randomness and efficiently sample the configuration space. The benefit of the SQS approach is that, since the SQS structures reproduce the most important correlations in a random mixture, the configuration space explored by SQSs represents the most probable chemical environments the defects may encounter in randomly disordered alloys. These states provide the dominant contributions to the thermal properties.

As the concentration of defects at thermal equilibrium (especially vacancies) is generally very low, it is reasonable to ignore the interactions among defects. In consequence, within the SQS approach, a single defect is generally introduced by removing (for vacancies) or adding (for impurities) an atom at one of the possible sites. The resulting defect supercell is subjected to self-consistent DFT relaxations to obtain total energies including local lattice



distortions. To achieve statistical sampling, this procedure is repeated for other defect sites in the same SQS supercell. For the defect migration energies, the DFT-based nudged elastic band (NEB) method (69, 70) is applied to two 'neighbor' defect supercells that are connected by images along the diffusion pathway in order to locate the saddle point.

By sampling sufficiently many defect energy states, the defect-DOS corresponding to the energetic property of interest can be obtained as exemplified in the blue box of Fig. 4. With the knowledge of the defect-DOS, the effective properties at finite temperatures can be accordingly extracted. For defect formation energies, previous studies have shown that a statistical analysis is required as the sampled energy states are not equally activated at finite temperatures (24, 71). The temperature-dependent 'configurational' excitations of defects result in negative formation entropies (71). The temperature-dependent defect concentrations exhibit a non-Arrhenius behaviour (24, 71).

**Cluster expansion technique.** The *ab initio* based cluster expansion (CE) technique has proven to be a very efficient and accurate tool to model alloy thermodynamics. It belongs to the category of lattice gas models with generalized mean-field approximations. Utilizing *ab initio* DFT energies as input, configuration-dependent energetic properties can be mapped onto Ising-like Hamiltonians with effective cluster interactions (ECIs). Several approaches are available for searching for a good CE and extracting the corresponding ECIs, as summarized in Ref. (72). Once a well-optimized CE is obtained, the associated ECIs can be used to predict energies of arbitrary configurations at low computational cost.

Originally, the CE technique was developed to mainly address phase stabilities related to order-disorder transitions and phase diagrams in binary alloys. Later, with the development of the local CE approach as well as the concept of the kinetically resolved activation (KRA) barriers, Van der Ven et al. investigated vacancies and interdiffusion in the  $\text{Li}_x\text{CoO}_2$  system (73) and binary Al-Li alloys (74, 75). By treating vacancies as an additional element, Zhang and Sluiter derived a statistical model coupled with a full ternary CE to study vacancy properties in disordered concentrated Cu-Ni alloys (76). Although being mainly applied to low-order systems, these successful extensions of the CE to diffusion energetics indicate the power of the CE to further model diffusion kinetics in multicomponent and multi-principal element systems. The applications of the CE to multicomponent diffusion, e.g., diffusion in HEAs, are limited due to the fact that the complexity of the CE parametrization significantly increases with increasing number of components and obtaining a good multicomponent CE becomes definitely non-trivial. Instead of a direct brute-force search in a multicomponent clusters pool, Zhang and Sluiter proposed a hierarchical approach to building up a multinary CE from ECIs of the subsystems with the concept of 'inheritance of expansion coefficients' (72). Such a promising feature may significantly reduce the difficulties of generating multicomponent CEs and provides a systematic way to establishing the *ab initio* alloy database analogous to the well-known CALPHAD approach. For vacancy migration barriers, it has been shown that special treatment, namely the introduction of the 'pseudoatomic pair' (as illustrated in Fig. 4 (d)), for the saddle-point configuration is necessary in order to retain the lattice gas assumption (72, 77).

## 6.2. Accurate vibrational free energies from machine learning potentials

The aforementioned defect configurational energetics does not include thermal vibration contributions. In reality, the diffusion processes (reorganizations of atoms) at elevated

temperatures are coupled with thermal excitations (atomic vibrations, electronic excitations etc.). Due to the fact that the time scale of thermal vibrations and diffusion are quite different, the vibrational contributions to the energetic properties can therefore be evaluated for a fixed atomic configuration. Nevertheless, *ab initio* calculations of the full temperature-dependent vibrational free energy including anharmonicity for a given atomic configuration with defects are highly demanding (78). With the aid of the recently-developed moment tensor potentials (MTPs, machine-learning based interatomic potentials), Grabowski et al. have developed an efficient computational framework based on the so-called 'TU-TILD' approach (79) for an efficient and accurate calculation of the full vibrational free energy of disordered multicomponent alloys (80). The MTPs have proven to be robust for describing different phases for a wide temperature and volume range, as shown in Fig. 4(g). The strong correlation of the DFT forces and MD forces predicted by MTP highlights the excellent performance of the MTP (see Fig. 4(h)).

### 6.3. Diffusion coefficients from kinetic Monte Carlo simulations

Fundamentally, diffusion processes at atomic scale can be described as a sequence of individual exchanges of vacancies with neighboring atoms or migrations of the interstitial impurity atoms. With the knowledge of the potential energy associated with each local minimum as well as the defects migration barriers, i.e., the potential energy surface on which the diffusing defects travel (illustrated in Fig. 4(i)), diffusion coefficients can be calculated by means of monitoring the displacements of different diffusing elements as a function of time in, e.g., kinetic Monte Carlo (KMC) or molecular dynamic (MD) simulations. All required energetics for describing the potential energy surface of diffusion in KMC can be provided via the CE parametrizations described in Sec. 6.1. In general, according to the formulas derived by Allnatt (81), the phenomenological Onsager coefficients;  $L_{ij}$ , can be calculated from the the ensemble average of the correlated fluctuations of species  $i$  and  $j$ , i.e.,

$$L_{ij} = \frac{\langle R_i R_j \rangle}{2dt} \quad 8.$$

where  $d$  is the lattice dimension,  $t$  is the time and  $R_{i(j)} = \sum_{k=1}^N r_{i(j)}^k$  with  $r_{i(j)}^k$  being the displacement of the  $k$ th atom of species  $i(j)$  and  $N$  the total number of species  $i(j)$ . By ignoring the cross correlations between different atoms, the Einstein formula for the tracer diffusion coefficient of species  $i$  is obtained, i.e.,

$$D_i^* = \frac{\langle R_i^2 \rangle}{2dt} \quad 9.$$

In order to compute the intrinsic diffusion coefficients and the interdiffusion coefficients, according to Eq. 4, thermodynamic factors—the second derivative of the free energy with respect to the element concentrations—have to be evaluated first. Besides the direct computation of the second derivatives, it has been shown that, for binaries, the grand canonical Monte Carlo simulation is an alternative approach for computing the thermodynamic factors (82).

The results of KMC simulations can directly be used to calculate the vacancy and atomic correlation factors (15, 32, 13). Using the random alloy model, these correlation factors have been determined for the equiatomic FCC CoCrFeMnNi alloy (13). The vacancy correlation factor was found to be less than unity, about 0.75 to 0.8 in the temperature interval of 1000 K to 1373 K (13). Such a value is consistent with some 'sluggishness' of diffusion in

### Supplemental information:

automated assessment of the mobility parameters

open-access software **PyMob**: <http://www.icams.de/content/software-development>

FCC HEAs with respect to the pure elements; though the analysis is still absent for BCC and HCP multi-principal element alloys.

## 7. CALPHAD MODELING OF MULTI-COMPONENT DIFFUSION

Within the last 30 years, CALPHAD method extended to mobility databases was successfully applied to assess the diffusion data following the phenomenological methodology similar to the thermodynamic description of Gibbs free energy for calculation of phase diagrams. Most important, the CALPHAD approach allows the extrapolation of the multicomponent diffusion data to unknown composition regions. A detailed overview of CALPHAD-type modeling of kinetic databases was given by Zhang and Chen (83). Here we discuss the recent advances in the modeling.

Before starting with the advances however, several major limitations for implementation of the CALPHAD method for diffusion processes have to be mentioned. First, the Darken approximation is followed for fluxes in a lattice-fixed reference frame. This approximation ignores all the jump correlation effects and can only be applied to the vacancy mechanism in the alloys with atomic mobilities that do not differ much from each other (moreover, the vacancy sources and sinks are not taken into account explicitly). This does not apply to intermetallic systems, where the diffusion rates of constituting elements can differ by orders of magnitude (37), and other (non-monovacancy) diffusion mechanisms. The second severe limitation is the simplification of the kinetic part of the interdiffusion problem, despite taking into account the influence of the vacancy wind (84). Since the thermodynamic part strongly influences the results, it is always necessary to make some corrections to the latter to ensure the correct effect of the thermodynamic data.

There are three main directions of developing of the CALPHAD-type mobility databases in the recent years. First is the thermodynamic assessment coupled with the interdiffusion coefficients extracted from diffusion couple and diffusion triple experiments (85), second is a new high-throughput technique of diffusion multiples coupled with the inverse numerical method (86), and third the direct extraction of the mobility parameters from the tracer diffusion experiments (87).

In (88, 89, 90) calorimetric experiments and *ab initio* calculations of end-member Gibbs energies are used to assess the thermodynamic properties of ternary Ni and Ti binary and ternary alloys. Then diffusion couples in conjunction to new thermodynamic database assessment were used to assess the atomic mobilities and CALPHAD-type mobility parameters. Diffusion couples of Ti triple systems were utilized to develop a self-consistent atomic mobility database in the works of Bai et al. (91, 92), Wei et al. (93), Dong et al. (94). Interdiffusion coefficients were extracted by the Whittle-Green method (95) and tracer diffusion coefficients by the Hall method (40). Diffusion couple experiments in the Fe-Al(Si Mn) bcc systems were used to optimize mobilities of the impurities Al, Si and Mn (96).

---

**CE:** cluster expansion

**ECI:** effective cluster interaction

**KRA:** kinetically resolved activation

**KMC:** kinetic Monte Carlo

**MD:** molecular dynamic

---

---

**CALPHAD:** CALculation of PHase Diagrams approach

**DICTRA:** Diffusion-Controlled TRAnsfOrmations - a tool for diffusion simulations

---

Similar experiments were carried out to extract the interdiffusion coefficients and impurity diffusion coefficients for the Mg-Li-Al system (97). The assessment of the thermodynamic parameters and mobility parameters was performed using the diffusion couple and diffusion triple experiments in the recent work of Xia et al. (85) in the Co-Fe-Ni system. The interdiffusion coefficients were extracted by the Sauer-Freise method (40). In all present works the DICTRA software withing ThermoCalc (<https://thermocalc.com>) was used to assess the mobility parameters from the chemical diffusion coefficients.

The concept of diffusion multiple was recently developed by Zhao et al. (98) which has an order of magnitude higher efficiency in comparison to diffusion couples. More details of can be seen in the review paper of Zhong (99). Recently the diffusion multiple method was used to assess the atomic mobilities in Fe-Mn-Si system (86) and five-component high-entropy alloys (HEA) by Chen and Zhang (100). The interdiffusivity matrices depending on the composition were prepared using the pragmatic inverse numerical method. The vacancy-wind effect was also taken into account. The authors used the end-member atomic mobility parameters known from the literature in order to assess the binary and ternary interaction parameters. In addition, the transformation relations between the diffusivities with different reference element were developed which are helpful for multi-principal element alloys. In application to the HEA, the mobility database was also developed using the literature data and validated by the diffusion experiments in the work of Zhang et al. (101).

In spite of the high efficiency of the diffusion multiple method, the definition of the atomic mobility parameters from interdiffusion coefficients is not very accurate, as discussed before, and because the results depend on the thermodynamic description of the system (85). In contrast, tracer diffusion experiments allow to define the mobility direct from the intrinsic diffusion coefficients using the Einstein relation and do not depend on the choice of the thermodynamic database. Moreover, tracer diffusion coefficients can give an important information about physical effects of the diffusion , e.g., effect of impurities or vacancies on the mobility of matrix components. For example, recently tracer diffusion experiments were carried out for Cr in Ni and Ni-Cr alloy by Gheno et al. (102) and the corresponding mobility parameters for the Ni-Cr system were re-assessed. Furthermore, the physical effect of the vacancy-solute exchange mechanism was found and studied.

A new method to be reported is the automated assessment of the mobility parameters from the tracer diffusion experiments the software PyMob (<http://www.icams.de/content/software-development>), developed by Abrahams et al. (87). A raw database of tracer diffusion coefficients is adopted to extract a database of mobility parameters. The parameters are assessed step by step from the end-members to the ternary interactions. The software allows quick update the database when new raw data become available. To choose the model variant with the corresponding mobility parameters the PyMob software uses statistical criteria, namely the Bayesian Information Criterion (BIC) and Akaike Information Criterion (AIC), to choose the model with or without ternary interactions. Note that DICTRA software allows also to assess the mobility parameters from different diffusion experiments, but one should learn how to implement the software to a specific case. For unknown end-member parameters, for example, for self-diffusion of Cr in (metastable) fcc lattice, one used the values calculated *ab initio* or by MD simulations.

As a last comment we would like to highlight the revision of the pair-exchange concept (103), which was applied together with the experimental tracer diffusion coefficients (see Sec. 5) to validate the thermodynamic database for HEAs applied to diffusion couple experiments (66). The pair-exchange formulation allows, in the framework of CALPHAD, a

unique definition of the diffusion coefficients of a multicomponent systems without specifying a reference chemical potential. Thereby the formal challenges in the description of the multi-principal element systems seem to be resolved.

## 8. SUMMARY AND CONCLUSIVE REMARKS

Tracer and intrinsic diffusion coefficients are the basic quantities required for quantitative understanding of the mass transport phenomena and diffusional interactions between components in complex multi-component material systems including multi-principal element and compositionally complex alloys. In this review, the latest developments related to the determination of these diffusion parameters from experimental, numerical-inverse and *ab initio*-informed methods have been discussed comprehensively.

The radiotracer method is a traditional and in principle straightforward technique for measuring the tracer diffusion coefficients of components in (typically homogeneous) alloys with fixed composition. The recently developed radiotracer-interdiffusion couple technique presents an advanced and unique approach to measure the concentration-dependent tracer diffusion coefficients in multi-components alloys paving the way to a high-throughput determination of the atomic mobilities. However, the tracer method faces serious problems with its application to several important constituting elements such as Al, Ga, Si, etc. because of the unavailability/short life times/high costs of the corresponding radioisotopes. Further, the usage of the radiotracer technique is nowadays limited due to stringent safety regulations.

The diffusion couple method is, therefore, a widely practiced alternative method. It used to be common textbook knowledge that, with the diffusion couple method, tracer and intrinsic diffusion coefficients could be estimated only for binary systems. For ternary systems, only the interdiffusion coefficients were accessible and no analytic expressions existed for the determination of the basic diffusion coefficients in systems with more than three components,  $n > 3$ . Nowadays, the recently proposed pseudo-binary (PB) method can be used to determine experimentally the tracer and main intrinsic diffusion coefficients of the components at the Kirkendall marker plane in an arbitrary multicomponent system. Tracer, main and cross intrinsic diffusion coefficients can be estimated by extending the Kirkaldy-Lane method proposed for ternary systems to pseudo-ternary (PT) and body-diagonal (BD) diffusion couples in multicomponent systems utilizing the thermodynamic details at the cross of the diffusion paths. Only two diffusion profiles are required irrespective of the number of components in an  $n > 2$  component system.

The combined radiotracer-interdiffusion couple method can be extended to PB, PT or BD diffusion couple methods for estimating the composition-dependent tracer and intrinsic diffusion coefficients for the whole composition interval of the diffusion path that develops during the measurement. Knowing the thermodynamic details, the tracer and intrinsic diffusion coefficients of the components for which suitable radioisotopes are not available can be furthermore determined. The experimental methods, being most suitable for homogeneous single-phase alloys, have their limitations and encounter obvious difficulties when applied to phase mixtures. Moreover, generation of composition-dependent diffusion parameters for all constituent components over a wide homogeneity range is not an easy task. As described, the PB, PT and BD methods work only when the diffusion profiles *can* be generated in some way in an actual measurement and may be restricted to a particular (not the whole) composition range of a system.

In the absence of available data or suitable experimental methods in a multicomponent system, the solution to determine the interdiffusion matrix was, in earlier times, established just from the measured concentration profiles. This is a serious drawback in the absence of the uniqueness of the solution. Today, these methods can be combined with the experimental methods for developing a reliable mobility database in complex material systems by comparing with the experimentally estimated tracer and intrinsic diffusion coefficients. Following this route, one can extract the data in a composition range in which the data cannot be estimated experimentally. In its current formulation, the Thermocalc-DICTRA method does not consider the contributions of the vacancy wind effect, which may play a crucial role and an alternate method is desirable. Recent advances in CALPHAD modeling of mobility databases for multicomponent alloys, including HEAs, and the new experimental methods and numerical techniques, which in principle can consider also the vacancy-wind effect, have been briefly described.

*Ab initio* density-functional-theory (DFT) based simulations have recently advanced to guide the design of novel multi-principal element alloys, e.g., predicting phase transitions and simulating diffusion properties. The main challenge lies in the fact that both highly-complex chemical and vibrational degrees of freedom need to be properly taken into account, requiring new methodological developments. We have shown in this review that the chemical degrees of freedom can be well tackled by highly optimized multi-component cluster expansions. Critical experimentally measurable diffusion coefficients, e.g., tracer and intrinsic diffusivities, can be extracted from direct kinetic Monte Carlo simulations or from the concentration profile analysis obtained from KMC. For the vibrational degrees of freedom, thermodynamic properties up to the melting point for HEAs can be efficiently calculated by the recently developed machine learning potentials with DFT accuracy. Most importantly, *ab initio* simulations at atomic scale provide physical insight into the interplay between phase stabilities and diffusion kinetics. Specifically, on the one hand, the change of the chemical order may have significant impact on the diffusion kinetics, e.g., the ultra-fast diffusion. On the other hand, interestingly, the specific diffusion kinetics may also result in different chemical short-range or long-range ordering.

To summarize, no method individually is enough to establish a reliable mobility database in a multicomponent alloy system of practical importance. A combination of experimental, numerical-inverse and DFT methods, as described in this review article, should be utilized to establish a reliable mobility database and the understanding of the complex diffusional interactions between the components to simulate the microstructural evolution or for understanding various physical and mechanical properties of materials.

## DISCLOSURE STATEMENT

The authors are not aware of any affiliations, memberships, funding, or financial holdings that might be perceived as affecting the objectivity of this review.

## ACKNOWLEDGMENTS

AP acknowledges the financial support from ARDB, India, Grant number: ARDB/GTMAP/01/2031786/M. Financial support from the Deutsche Forschungsgemeinschaft (DFG) via the research projects DI 1419/13-1, DI 1419/17-1, GR 3716/5-1, and STE 116/30-1/2 is gratefully acknowledged. BG acknowledges the funding from the

European Research Council (ERC) under the EU's Horizon 2020 Research and Innovation Programme (Grant No. 865855) and the support by the Stuttgart Center for Simulation Science (SimTech).

## LITERATURE CITED

1. Miracle D, Senkov O. 2017. A critical review of high entropy alloys and related concepts. *Acta Materialia* 122:448–511
2. Cantor B, Chang I, Knight P, Vincent A. 2004. Microstructural development in equiatomic multicomponent alloys. *Materials Science and Engineering: A* 375–377:213–218
3. Senkov O, Scott J, Senkova S, Miracle D, Woodward C. 2011. Microstructure and room temperature properties of a high-entropy TaNbHfZrTi alloy. *J Alloys Compounds* 509:6043–6048
4. Feuerbacher M, Lienig T, Thomas C. 2018. A single-phase bcc high-entropy alloy in the refractory Zr–Nb–Ti–V–Hf system. *Scripta Materialia* 152:40–43
5. Feuerbacher M, Heidelmann M, Thomas C. 2016. Hexagonal High-entropy Alloys. *Materials Research Letters* 3:1–6
6. Rogal L, Bobrowski P, Körmann F, Divinski S, Stein F, Grabowski B. 2017. Computationally-driven engineering of sublattice ordering in a hexagonal AlHfScTiZr high entropy alloy. *Scientific Reports* 7:1–14
7. Yeh J, Chen S, Lin S, Gan J, Chin T, et al. 2004. Nanostructured high-entropy alloys with multiple principal elements: Novel alloy design concepts and outcomes. *Adv. Eng. Mater.* 6:299–303
8. Divinski S, Lukianova O, Wilde G, Dash A, Esakkiraja N, Paul A. 2020. High-entropy alloys: Diffusion. *Encyclopedia of Materials: Science and Technology*
9. Dabrowa J, Zajusz M, Kucza W, Cieslak G, Berent K, et al. 2019. Demystifying the sluggish diffusion effect in high entropy alloys. *Journal of Alloys and Compounds* 783:193207
10. Mehta A, Sohn Y. 2021. Investigation of sluggish diffusion in FCC  $Al_{0.25}CoCrFeNi$  high-entropy alloy. *Materials Research Letters* 9(5):239–246
11. Mehrer H. 1990. *Diffusion in Solids. Fundamentals, Methods, Materials, Diffusion-Controlled Processes*. Springer, Berlin
12. Vaidya M, Pradeep K, Murty B, Wilde G, Divinski S. 2018. Bulk tracer diffusion in CoCrFeNi and CoCrFeMnNi high entropy alloys. *Acta Materialia* 146:211–224
13. Gaertner D, Kottke J, Chumlyakov Y, Hergemller F, Wilde G, Divinski SV. 2020. Tracer diffusion in single crystalline CoCrFeNi and CoCrFeMnNi high-entropy alloys: Kinetic hints towards a low-temperature phase instability of the solid-solution? *Scripta Materialia* 187:57–62
14. Paul A, Laurila T, Vuorinen V, Divinski SV. 2014. *Thermodynamics, diffusion and the Kirkendall effect in solids*. Springer
15. Murch GE, Thorn RJ. 1979. Calculation of the diffusion correlation factor by monte carlo methods. *Phil Mag A* 39:673–677
16. Mizuno M, Sugita K, Araki H. 2019. Defect energetics for diffusion in crmnfeconi high-entropy alloy from first-principles calculations. *Comput. Mater. Sci* 170:109163
17. Quyang H. and Fultz B. 1989. Percolation in alloys with thermally activated diffusion. *Journal of Applied Physics* 66:4752–4755
18. Maier K, Mehrer H, Lessmann E, Schuele W. 1976. Self-diffusion in nickel at low temperatures. *Phys Status Solidi B* 78:689–698
19. James D, Leak G. 1966. Self-diffusion and diffusion of cobalt in alpha and delta-iron. *Philosophical Magazine* 14:701–713
20. Hood G, Zou H, Schultz R, Matsuura N, Roy J, Jackman J. 1997. Self- and Hf diffusion in  $\alpha$ -Zr and in dilute, Fe-free, Zr(Ti) and Zr(Nb) alloys. *Defect Diff Forum* 143:49–54
21. Million B, Rikov J, Velek J, Vel J. 1981. Diffusion processes in the Fe–Ni system. *Materials*

*Science and Engineering* 50(1):43–52

22. Iijima Y, Kimura K, Lee CG. 1995. Self-diffusion in bcc and ordered phases of an equiatomic iron-cobalt alloy. *Acta Metal. Mater.* 43:1183–1188
23. Nadutov V, Mazanko V, Makarenko S. 2017. Tracer diffusion of cobalt in high-entropy alloys  $\text{Al}_x\text{FeNiCoCuCr}$ . *Metallofizika i Noveishie Tekhnologii* 39:337–348
24. Vaidya M, Sen S, Zhang X, Frommeyer L, Rogal L, et al. 2020. Phenomenon of ultra-fast tracer diffusion of Co in HCP high entropy alloys. *Acta Materialia* 196:220–230
25. Zhang J, Muralikrishna GM, Asabre A, Kalchev Y, Mller J, et al. 2021. Tracer diffusion in the  $\sigma$  phase of the CoCrFeMnNi system. *Acta Metallurgica* 203:116498
26. Frank S, Sdervall U, Herzig C. 1995. Self-Diffusion of Ni in Single and Polycrystals of  $\text{Ni}_3\text{Al}$ . A Study of SIMS and Radiotracer Analysis. *Phys. Stat. Sol.* 191(b):45–55
27. Knorr K, Macht M, Freitag K, Mehrer H. 1999. Self-diffusion in the amorphous and supercooled liquid state of the bulk metallic glass  $\text{Zr}_{46.75}\text{Ti}_{8.25}\text{Cu}_{7.5}\text{Ni}_{10}\text{Be}_{27.5}$ . *Journal of Non-Crystalline Solids* 250–252(2):669–673
28. Kstler C, Faupel F, Hehenkamp T. 1986. Carbon-vacancy binding in Ni–C alloys. *Scripta Metallurgica* 20:1755–1759
29. Chen T, Tiwari GP, Iijima Y, Yamauchi K. 2003. Volume and Grain Boundary Diffusion of Chromium in Ni-Base NiCrFe Alloys. *Materials Transactions* 44(1):40–46
30. Lukianova O, Rao Z, Kulitckii V, Li Z, Wilde G, Divinski S. 2020. Impact of interstitial carbon on self-diffusion in CoCrFeMnNi high entropy alloys. *Scripta Materialia* 188:264–268
31. Mehrer H, ed. 1990. in: *Landolt-Börnstein, Numerical Data and Functional Relationships in Science and Technology, New Series, Group III: Crystal and Solid State Physics, Vol. 26, Diffusion in Metals and Alloys*. Springer
32. Kottke J, Utt D, Laurent-Brocq M, Fareed A, Gaertner D, et al. 2020. Experimental and theoretical study of tracer diffusion in a series of  $(\text{CoCrFeMn})_{100-x}\text{Ni}_x$  alloys. *Acta Materialia* 194:236–248
33. Vaidya M, Trubel S, Murty B, Wilde G, Divinski S. 2016. Ni tracer diffusion in CoCrFeNi and CoCrFeMnNi high entropy alloys. *Journal of Alloys and Compounds* 688:994–1001
34. Herzig C, Willecke R, Vieregge K. 1991. Self-diffusion and fast cobalt impurity diffusion in the bulk and in grain boundaries of hexagonal titanium. *Philosophical Magazine A* 63:949–958
35. Wang Q, Lu Y, Yu Q, Zhang Z. 2018. The Exceptional Strong Face-centered Cubic Phase and Semi-coherent Phase Boundary in a Eutectic Dual-phase High Entropy Alloy AlCoCrFeNi. *Sci Rep* 8:14910
36. Tsai K, Tsai M, Yeh J. 2013. Sluggish diffusion in Co–Cr–Fe–Mn–Ni high-entropy alloys. *Acta Materialia* 61:48874897
37. Divinski S. 2017. *Defects and diffusion in ordered compounds (Chapter 10) in: A. Paul, S.V. Divinski (ed) Handbook of Solid State Diffusion: Volume 1, Diffusion Fundamentals and Techniques*. Elsevier
38. He Q, Y. Y, Yang Y. 2017. Formation of random solid solution in multicomponent alloys: from Hume-Rothery rules to entropic stabilization. *J Phase Equilib Diffus.* 38:416425
39. Faupel F, Frank W, Macht MP, Mehrer H, Naundorf V, et al. 2003. Diffusion in metallic glasses and supercooled melts. *Rev Modern Phys* 75:237–280
40. Paul A, Divinski S. 2017. *Handbook of Solid State Diffusion: Volume 1: Diffusion Fundamentals and Techniques*, vol. 1. Elsevier
41. Manning JR. 1970. Cross terms in the thermodynamic diffusion equations for multicomponent alloys. *Metallurgical and Materials Transactions B* 1(2):499–505
42. Manning J. 1967. Diffusion and the kirkendall shift in binary alloys. *Acta Metallurgica* 15(5):817–826
43. Darken LS. 1948. Diffusion, mobility and their interrelation through free energy in binary metallic systems. *Trans. Aime* 175:184–201
44. Le Claire A. 1958. Random walks and drift in chemical diffusion. *Philosophical Magazine*



- 3(33):921–939
45. Onsager L. 1931. Reciprocal relations in irreversible processes. ii. *Physical review* 38(12):2265
  46. Onsager L. 1945. Theories and problems of liquid diffusion. *Annals of the New York Academy of Sciences* 46(5):241–265
  47. Esakkiraja N, Dash A, Mondal A, Hary Kumar K, Paul A. 2021. Correlation between estimated diffusion coefficients from different types of diffusion couples in multicomponent system. *Materialia* 16:101046
  48. Kirkaldy JS, Young DJ. 1987. Diffusion in the condensed state. *The Institute of Metals, 1 Carlton House Terrace, London SW 1 Y 5 DB, UK, 1987.*
  49. Kirkaldy J, Lane J. 1966. Diffusion in multicomponent metallic systems: Ix. intrinsic diffusion behavior and the kirkendall effect in ternary substitutional solutions. *Canadian Journal of Physics* 44(9):2059–2072
  50. Cserháti C, Ugaste Ü, Van Dal M, Lousberg N, Kodentsov A, van Loo F. 2001. On the relation between interdiffusion and tracer diffusion coefficients in ternary solid solutions. *Defect and Diffusion Forum* 194:189–194
  51. Paul A. 2013. A pseudobinary approach to study interdiffusion and the kirkendall effect in multicomponent systems. *Philosophical Magazine* 93(18):2297–2315
  52. Esakkiraja N, Pandey K, Dash A, Paul A. 2019. Pseudo-binary and pseudo-ternary diffusion couple methods for estimation of the diffusion coefficients in multicomponent systems and high entropy alloys. *Philosophical Magazine*
  53. Dash A, Esakkiraja N, Paul A. 2020. Solving the issues of multicomponent diffusion in an equiatomic niofocer medium entropy alloy. *Acta Materialia* 193:163–171
  54. Paul A. 2017. Comments on Sluggish diffusion in Co–Cr–Fe–Mn–Ni high-entropy alloys by KY Tsai, MH Tsai and JW Yeh, *Acta Materialia* 61 (2013) 4887–4897. *Scripta Materialia* 135:153–157
  55. Esakkiraja N, Gupta A, Jayaram V, Hickel T, Divinski SV, Paul A. 2020. Diffusion, defects and understanding the growth of a multicomponent interdiffusion zone between Pt-modified B2 NiAl bond coat and single crystal superalloy. *Acta Materialia* 195:35–49
  56. Kiruthika P, Paul A. 2015. A pseudo-binary interdiffusion study in the  $\beta$ -Ni (Pt) Al phase. *Philosophical Magazine Letters* 95(3):138–144
  57. Kiruthika P, Makineni S, Srivastava C, Chattopadhyay K, Paul A. 2016. Growth mechanism of the interdiffusion zone between platinum modified bond coats and single crystal superalloys. *Acta Materialia* 105:438–448
  58. DeHoff R, Kulkarni N. 2002. The trouble with diffusion. *Materials Research* 5(3):209–229
  59. Morral JE. 2018. Body-diagonal diffusion couples for high entropy alloys. *Journal of Phase Equilibria and Diffusion* 39(1):51–56
  60. Verma V, Tripathi A, Venkateswaran T, Kulkarni KN. 2020. First report on entire sets of experimentally determined interdiffusion coefficients in quaternary and quinary high-entropy alloys. *Journal of Materials Research* 35(2):162–171
  61. Esakkiraja N, Paul A. 2018. A novel concept of pseudo ternary diffusion couple for the estimation of diffusion coefficients in multicomponent systems. *Scripta Materialia* 147:79–82
  62. Manning JR. 1959. Tracer diffusion in a chemical concentration gradient in silver-cadmium. *Physical Review* 116:69–80
  63. Meyer R, Slifkin L. 1966. Activity coefficient and vacancy-flow effects on diffusion in silver-gold alloys. *Physical Review* 149:556–563
  64. Belova I, Kulkarni N, Sohn Y, Murch G. 2014. Simultaneous tracer diffusion and interdiffusion in a sandwich-type configuration to provide the composition dependence of the tracer diffusion coefficients. *Philosophical Magazine* 94:3560–3573
  65. Belova I, Sohn Y, Murch G. 2015. Measurement of tracer diffusion coefficients in an interdiffusion context for multicomponent alloys. *Philosophical Magazine Letters* 95:416424
  66. Gaertner D, Abrahams K, Kottke J, Esin VA, Steinbach I, et al. 2019. Concentrationdependent

- atomic mobilities in fcc cocrfemnni hightentropy alloys. *Acta Materialia* 166
67. Muralikrishna G, Tas B, Esakkiraja N, Esin V, Hari Kumar K, et al. 2021. Composition dependence of Fe tracer diffusion coefficients in FeGa alloys: a case study by a tracer-interdiffusion couple method. *Acta Materialia* 203:116446
  68. Zunger A, Wei SH, Ferreira LG, Bernard JE. 1990. Special quasirandom structures. *Phys. Rev. Lett.* 65(3):353–356
  69. Henkelman G, Uberuaga BP, Jónsson H. 2000. A climbing image nudged elastic band method for finding saddle points and minimum energy paths. *The Journal of Chemical Physics* 113(22):9901–9904
  70. Henkelman G, Jónsson H. 2000. Improved tangent estimate in the nudged elastic band method for finding minimum energy paths and saddle points. *The Journal of Chemical Physics* 113(22):9978–9985
  71. Zhang X, Divinski SV, Grabowski B. 2021. Ab initio prediction of vacancy energetics in HCP Al-Hf-Sc-Ti-Zr high entropy alloys and the subsystems. *to be published*
  72. Zhang X, Sluiter MHF. 2016. Cluster expansions for thermodynamics and kinetics of multi-component alloys. *Journal of Phase Equilibria and Diffusion* 37(1):44–52
  73. Van der Ven A, Ceder G, Asta M, Tepeš PD. 2001. First-principles theory of ionic diffusion with nondilute carriers. *Phys. Rev. B* 64(18):184307
  74. Van der Ven A, Ceder G. 2005. Vacancies in ordered and disordered binary alloys treated with the cluster expansion. *Phys. Rev. B* 71(5):054102
  75. Van der Ven A, Ceder G. 2005. First principles calculation of the interdiffusion coefficient in binary alloys. *Physical Review Letters* 94(4):045901
  76. Zhang X, Sluiter MHF. 2015. Ab initio prediction of vacancy properties in concentrated alloys: The case of fcc Cu-Ni. *Phys. Rev. B* 91(17):174107
  77. Zhang X, Sluiter MHF. 2019. Kinetically driven ordering in phase separating alloys. *Phys. Rev. Materials* 3(9):095601
  78. Zhang X, Grabowski B, Hickel T, Neugebauer J. 2018. Calculating free energies of point defects from ab initio. *Computational Materials Science* 148:249–259
  79. Duff AI, Davey T, Korbmacher D, Glensk A, Grabowski B, et al. 2015. Improved method of calculating ab initio high-temperature thermodynamic properties with application to zrc. *Phys. Rev. B* 91(21):214311
  80. Grabowski B, Ikeda Y, Srinivasan P, Körmann F, Freysoldt C, et al. 2019. Ab initio vibrational free energies including anharmonicity for multicomponent alloys. *npj Computational Materials* 5(1):80
  81. Allnatt AR. 1965. Theory of phenomenological coefficients in solidstate diffusion. i. general expressions. *The Journal of Chemical Physics* 43(6):1855–1863
  82. Van der Ven A, Yu HC, Ceder G, Thornton K. 2010. Vacancy mediated substitutional diffusion in binary crystalline solids. *Progress in Materials Science* 55(2):61–105
  83. Zhang L, Chen Q. 2017. Chapter 6 - calphad-type modeling of diffusion kinetics in multicomponent alloys. In *Handbook of Solid State Diffusion, Volume 1*, ed. A Paul, S Divinski, pp. 321–362. Elsevier
  84. Manning J. 1968. *Diffusion Kinetics for Atoms in Crystals*. Princeton: Van Nostrand
  85. Xia CH, Wang Y, Wang JJ, Lu XG, Zhang L. 2021. Thermodynamic assessment of the CoFeNi system and diffusion study of its fcc phase. *Journal of Alloys and Compounds* 853:157165
  86. Deng S, Chen W, Zhong J, Zhang L, Du Y, Chen L. 2017. Diffusion study in bcc A2 Fe-Mn-Si system: Experimental measurement and CALPHAD assessment. *Calphad* 56:230–240
  87. Abrahams K, Zomorodpoosh S, Khorasgani AR, Roslyakova I, Steinbach I, Kundin J. 2021. Automated assessment of a kinetic database for fcc CoCrFeMnNi high entropy alloys. *Modelling Simul. Mater. Sci. Eng.* 29:0550072
  88. Zhao N, Liu W, Wang JJ, Lu XG, Zhang L. 2020. Thermodynamic assessment of the NiCoCr system and Diffusion Study of its fcc phase. *Calphad* 71:101996

89. Wang J, Zheng W, Xu G, Zeng X, Cui Y. 2020. Thermodynamic assessment of the TiAlZr system and atomic mobility of its bcc phase. *Calphad* 70:101801
90. Jinwan H, Yang W, Jingjing W, Xiao-Gang L, Lijun Z. 2018. Thermodynamic Assessments of the Ni-Cr-Ti System and Atomic Mobility of Its fcc Phase. *Journal of Phase Equilibria and Diffusion* 39:597–609
91. Bai W, Tian Y, Xu G, Yang Z, Liu L, et al. 2019. Diffusivities and atomic mobilities in bcc Ti-Zr-Nb alloys. *Calphad* 64:160–174
92. Bai W, Xu G, Tan M, Yang Z, Zeng L, et al. 2018. Diffusivities and Atomic Mobilities in bcc Ti-Mo-Zr Alloys. *Materials* 11(10)
93. Wei Z, Wang C, and Yong Lu SQ, Yu X, Liu X. 2020. Assessment of Atomic Mobilities for bcc Phase in the Ti-Nb-V System. *J. Phase Equilib. Diffus.* 41:191–206
94. Dong H, Wang J, Xu G, Zhou L, Cui Y. 2018. Assessment of atomic mobility for BCC Ti-Mn and Ti-Al-Mn alloys. *Calphad* 62:141–147
95. Whittle D, Green A. 1974. The measurement of diffusion coefficients in ternary system. *Scripta Metallurgica* 8:883–884
96. Zheng W, Wang J, He Y, Lu XG, Li L. 2018. Experimental and computational study of diffusion mobilities for the bcc phase in the Fe-Al-(Si, Mn) systems. *Calphad* 61:189–197
97. Christianson DW, Zhu L, Manuel MV. 2020. Experimental measurement of diffusion coefficients and assessment of diffusion mobilities in HCP MgLiAl alloys. *Calphad* 71:101999
98. Zhao JC, Zheng X, Cahill DG. 2005. High-throughput diffusion multiples. *Materials Today* 8(10):28–37
99. Zhong J, Chen L, Zhang L. 2020. High-throughput determination of high-quality interdiffusion coefficients in metallic solids: a review. *Journal of Materials Science* *Journal of Materials Science* 55:10303–10338
100. Chen W, Zhang L. 2017. High-throughput determination of interdiffusion coefficients for CoCr-FeMnNi high-entropy alloys. *J Phase Equilib Diffus* 38:457–465
101. Zhang C, Zhang F, Jin K, Bei H, Chen S, et al. 2017. Understanding of the elemental diffusion behavior in concentrated solid solution alloys. *J. Phase Equilib. Diffus.* 38:434–444
102. Gheno T, Jomard F, Desgranges C, Martinelli L. 2018. Tracer diffusion of Cr in Ni and Ni–22Cr studied by SIMS. *Materialia* 3:145–152
103. Kundin, J. and Steinbach, I. and Abrahams, K. and Divinski, S. V. 2021. Pair-exchange diffusion model for multicomponent alloys revisited. *Materialia* 16